

---

---

## International Journal of Bio-Inorganic Hybrid Nanomaterials

---

---

# Simple Photovoltaic Device Based on Multiwall Carbon Nanotube/Silicon Heterojunction

Luca Camilli, Manuela Scarselli, Silvano Del Gobbo, Paola Castrucci  
and M. De Crescenzi\*

*Dipartimento di fisica, Università di Roma Tor Vergata. Via della Ricerca Scientifica,  
1-Rome 00133-Italy*

Received: 20 January 2012; Accepted: 22 March 2012

---

### ABSTRACT

Multiwall carbon nanotubes (MWCNTs) are grown via chemical vapour deposition method directly on a stainless steel substrate. Raman spectroscopy and transmission electron microscopy are the techniques chosen to characterize the structure of the synthesized carbon nanotubes: few structural defects are detected. After their removal from the stainless steel substrate, the as-grown MWCNTs are then airbrushed on a crystalline n-type silicon substrate to build up a simple photovoltaic device based on the MWCNT/Si Schottky heterojunction. Several devices have been made up by varying the thickness of the MWCNT film. External quantum efficiency (EQE) measurements performed in planar configuration show that Si substrate plays the major role in the generation of the electron-hole pairs upon illumination. For this reason, the EQE lineshape closely resembles the behaviour of a p-n junction solar cell. In addition, a sizeable variation of the EQE as a function of the MWCNT film thickness is observed. On-off cycles, performed on the device showing the larger value of EQE (18%), illustrate the genuine photovoltaic effect of our MWCNT/Si device.

**Keyword:** Carbon nanotubes; CVD growth; MWCNT/Si heterojunction; photovoltaic effect; structural properties.

---

### 1. INTRODUCTION

Multiwall carbon nanotubes (MWCNTs) consist of multiple layers of graphite sheets forming concentric cylinders. The number of concentric cylinders in a MWCNT can vary from two to many tens. A

few years ago we showed the ability of MWCNTs to generate photocurrent in an electrochemical cell with an incident photon to current efficiency (IPCE) higher [1] than that measured for single wall

---

(\*) Corresponding Author - e-mail: decrescenzi@roma2.infn.it

carbon nanotubes (SWCNTs) by Kamat and co-workers [2]. In the same period and in the following years, other papers showed that MWCNTs can generate photocurrent as well [3-5]. Nonetheless, the mechanism of carrier photo-generation in MWCNTs and transport still remain an open question.

Here we show that MWCNTs exhibit an interesting photovoltaic activity when they are air-brushed on a crystalline n-type silicon substrate. We demonstrate that the external quantum efficiency (EQE) of the device, measured in planar geometry, is strongly dependent on the thickness and, as a consequence, on the resistance of the MWCNT film. This finding is consistent with previous results obtained in case of single wall [6] and multi wall carbon nanotubes [7]. The EQE extends over the visible and near ultraviolet wavelength range (down to 300 nm) and reaches a maximum of 18%, located at about 790 nm.

## 2. EXPERIMENTAL

### *Materials and methods*

A piece of AISI 316-stainless steel (30×40 mm<sup>2</sup>, from Goodfellow Cambridge Ltd.) is mounted on a resistive sample holder and inserted into the chemical vapour deposition chamber. After air is removed by a rotary pump, argon gas (12 torr) is inserted. When the desired temperature is reached (750°C), acetylene gas flows (200 sccm) in the chamber, thus starting the MWCNT growth. After 10 min, acetylene flow is stopped and argon (500 sccm) is inserted for 5 min to stop the reaction, while the chamber is cooling down to room temperature. More details are reported elsewhere [8].

Raman spectroscopy is employed to characterize the synthesized sample. The Raman spectra are obtained by a micro-Raman setup equipped with Rayleigh scattering micro imaging. The setup is made up of a Coherent Sabre Ar<sup>+</sup> laser, a Dilor triple monochromator equipped with LN<sub>2</sub> cooled CCD (Horiba 3000C), confocal optics and a nanometric piezo actuated positioning/scanning table. The confocal optics allows a spatial resolution of

~350 nm in the xy plane and of ~1 μm along the z-axis. The spectrum is acquired using an exciting laser wavelength of 514 nm in the backscattering configuration z(x,x)-z.

The morphology and structure of the MWCNTs are examined using a cold FEG Hitachi HF2000 transmission electron microscope (TEM) operated at 200 kV. In order to collect images from the self-supported nanostructures, TEM samples were prepared scratching with a razor blade the synthesis product from the SS surface directly on a gold TEM grid (mesh 1000).

In order to detach the MWCNTs from the steel substrate after the growth, the sample is sonicated in isopropyl alcohol. The obtained solution is then airbrushed on a patterned n-Si/SiO<sub>2</sub> substrate. The SiO<sub>2</sub> steps are needed to prevent short circuits between the metallic electrodes and the Si underneath (Figure 1). The airbrushed MWCNTs form a quasi continuous film that creates the photoactive Schottky heterojunction with the Si. The two electrodes are made of silver paint. The photocurrent spectra are measured using an optical set-up made up of a xenon lamp equipped with a monochromator, focusing and collecting optics, a reflecting chopper and lock-in electronics. The light spot size is (1×2) mm<sup>2</sup>. The photocurrent density, I(λ), is measured under illumination as a function of the incident photon wavelength, λ. The incident photon power density is monitored with a calibrated silicon photodiode and data are collected by a lock-in technique. The external quantum efficiency (EQE) is defined as the fraction of the incident photons, N<sub>ph</sub>, converted into photocurrent, i.e. the number of the generated e-h pairs, Ne-h, multiplied by the electronic charge, e. The number of the incident photons is then evaluated in terms of the power density of the Xe lamp, P(λ), since N<sub>ph</sub> = λP(λ)/hc. Therefore, it results:

$$EQE(\%) = \frac{\text{electrons}}{\text{photons}} = \frac{100 hcI(\lambda)}{e\lambda P(\lambda)}$$

I(λ) is measured by modulating the light by an optical chopper and recovering the amplified current signal (converted to voltage) by a lock-in

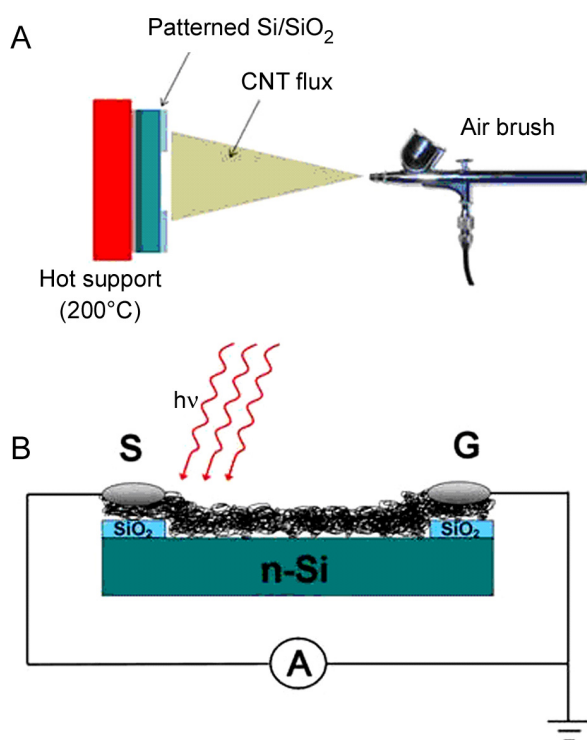


**Figure 1:** A) Schematic depiction of the airbrush deposition process. The solution of MWCNTs in isopropilic alcohol is airbrushed on a Si/SiO<sub>2</sub> sample. The SiO<sub>2</sub> steps avoid short circuit between top electrodes and Si. The Si window is 5×5 mm<sup>2</sup>. During airbrushing, the device is mounted on an heatable holder (~200°C) in order to allow a sudden evaporation of the solvent thus avoiding formation of drops. B) Scheme of the device used to perform photocurrent measurements. Note the planar geometry of the metallic contacts (silver paint). Steps of SiO<sub>2</sub> (300 nm) are used to avoid the electrical contact between silver paint and the silicon substrate. S denotes the electrode where the signal is measured while G is the grounded electrode.

amplifier locked on the chopper frequency and the lamp power  $P(\lambda)$  is measured simultaneously in a similar way by a calibrated Si photodiode;  $h$  is the Planck constant,  $c$  is the speed of light in vacuum and  $e$  the electron charge. Finally, using a Keithley 2602A sourcemeter, we record on-off cycles under white light illumination. More details on the experimental apparatus can be found elsewhere [5].

EQE spectra were acquired for samples with

different thickness of airbrushed CNT film deposited on n-Si crystalline substrates.

### 3. RESULTS AND DISCUSSION

In Figure 2 is reported the Raman spectrum acquired on the as-grown MWCNTs. Well-known D and G peak are observed near 1360, 1590 cm<sup>-1</sup>. The arrow shows the feature located at higher energy with respect to the G band and it is characteristic of the formation of multi walled structure. Although it is now known that the origin of the D peak is due to a double resonance, not just due to phonon confinement, its intensity can still be related to inter-defect distances in the carbon structure [9]. In particular, smaller values for the  $I_D/I_G$  ratio infer larger inter-defect distances in graphite structures [10,11]. In our case, the intensity of the D-band results in being about one third of the G-band feature. Using the formula given by Tuinstra and Koenig [10] the inter-defect distances was estimated of about 14.5 nm, thus suggesting that our carbon nanotubes are characterized by very few structural imperfections.

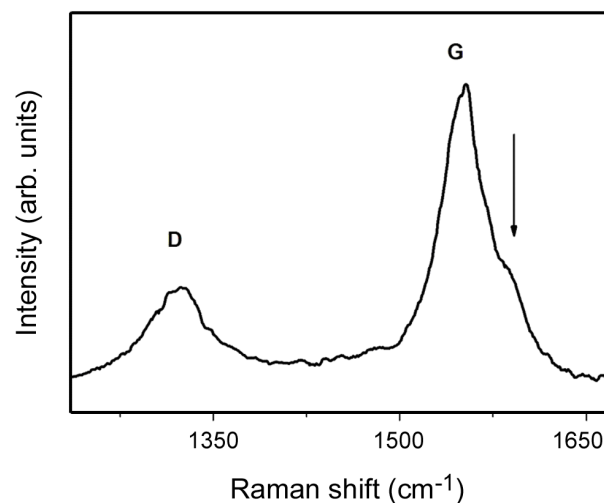


**Figure 2:** Raman spectrum of MWCNTs grown on SS sheet. The D-band intensity is almost one third of G-band feature, proving high structural quality of the sample. The arrow shows the feature located at higher energy with respect to the G band and it is characteristic of the formation of multi walled structure.

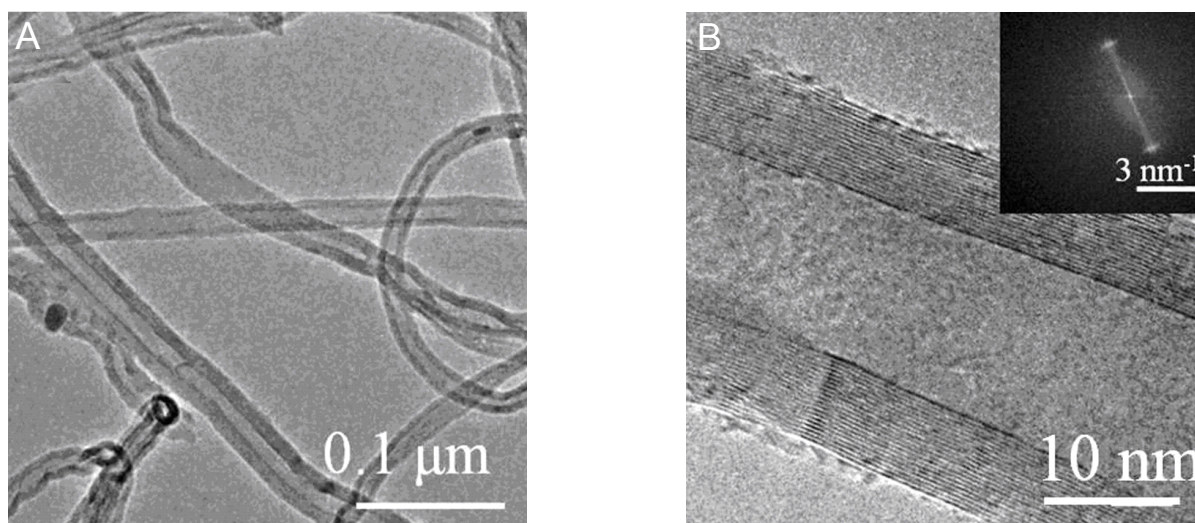


**Figure 3:** A) TEM image of the MWCNT synthesized on stainless steel via CVD. B) Blow up of a single MWCNT. Inset: Fast Fourier Transform of image 3B.

TEM images prove the multi walled nature of carbon nanotubes with an average number of walls of about 20, as reported in Figure 3A. The high graphitization degree of the synthesized nanostructures is evidenced by the Fast Fourier

Transform in Figure 3B.

The EQE spectra of our photovoltaic device, based on the MWCNT/Si heterojunction, extend over all the visible and near ultraviolet wavelength range (down to 300 nm), as showed in Figure 4.

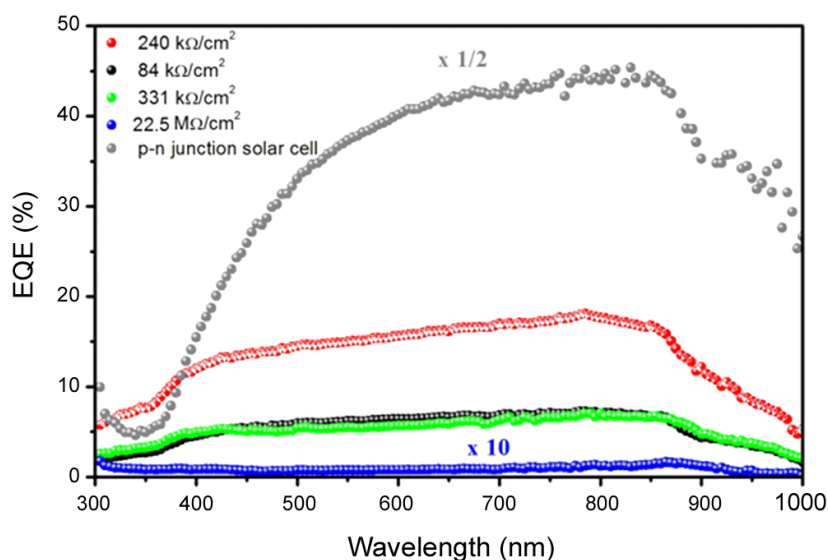


**Figure 4:** EQE of MWCNT random networks deposited by airbrush on a n-type Si substrate. Figure 4. EQE of MWCNT random networks deposited by airbrush on a n-type Si substrate. The resistivity (measured between the two metallic electrodes) of the several MWCNTs samples is reported and it is proportional to inverse of the film thickness. The blue curve has been obtained for a very thin film. In order to report all the curves on the same scale, the grey curve and the blue one are multiplied for a factor 1/2 and 10 respectively.

Interestingly, we observe a sizeable variation of the EQE as a function of the MWCNT film thickness. We report the EQE as a function of resistivity of the samples ( $\rho$ ). The value of the resistivity is proportional to the inverse of the thickness of the MWCNT film and it is chosen as reference parameter because the intrinsic inhomogeneity of the nanostructured film height. However, from SEM images, we have estimated that the film thickness ranges between 50 nm to 500 nm. Beginning with the thickest sample ( $\rho = 84 \text{ k}\Omega/\text{cm}^2$ , green curve), we observe an EQE value of 7% at 790 nm, then an increase up to 18% for a sample with  $\rho = 240 \text{ k}\Omega/\text{cm}^2$  (red curve) and a marked decrease for thinner ones ( $\rho = 331 \text{ k}\Omega/\text{cm}^2$  and  $22.5 \text{ M}\Omega/\text{cm}^2$ ), shown as black and blue curves respectively. The blue curve shows the same line shape of the other curves but its maximum value is only 0.2 % (note that in the figure the blue curve is multiplied by a factor of 10 for clarity purposes). This behavior suggests the existence of an optimum thickness value of the MWCNT network for which the EQE achieves its maximum value. This is consistent with the results reported for a similar device built with single wall [6] and multi wall carbon nanotubes [7]. Indeed, the EQE dependence on the MWCNT film thickness must be interpreted as following: carbon nanotube network should be thick enough to have the highest number of heterojunctions formed (among the MWCNTs and silicon substrate) and thin enough to not absorb too much the incident light, thus preventing the illumination of the silicon substrate underneath. The impinging of the light on the silicon substrate is mandatory for a high value of EQE since the Si is the main actor for generation of electron-hole pairs. This idea is confirmed when one compares the EQE lineshape obtained from our device with that obtained from a p-n polycrystalline Si solar cell.

One can observe that the presented photovoltaic device shows a EQE response between 450 nm and 850 nm flatter than that of the p-n junction solar cell. This finding is ascribed to a partial light absorption of MWCNT film [12], thus preventing the illumination of the Si. This behaviour implies that the MWCNT film acts mainly as semi-

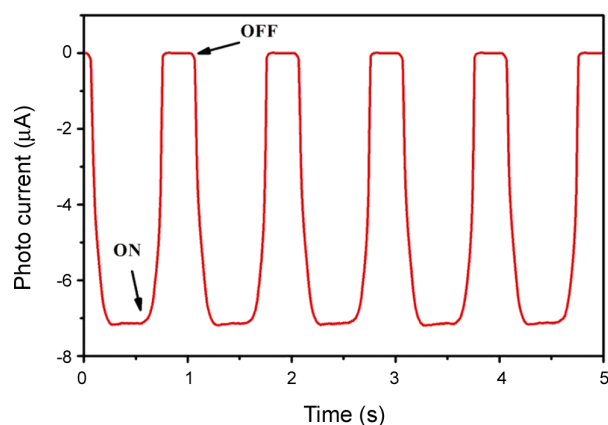


**Figure 5:** On-off cycles recorded under white light illumination (Xe lamp,  $\sim 80 \text{ mW}/\text{cm}^2$ ). This on-off cycles are related to sample with CNT film resistivity ( $\rho$ ) of  $240 \text{ k}\Omega/\text{cm}^2$ .

transparent electrode and to a lesser extent as photoactive layer. On the other hand, our device shows a high EQE response also below 350 nm, due to the continuous absorption toward higher energies of the MWCNTs [12]. In the same spectral region the p-n junction solar cell is less efficient because the Si absorption is poor [13].

Figure 5 displays typical on-off cycles recorded under white light illumination for the device that showed the largest value of EQE, thus proving a genuine photocurrent generation.

#### 4. CONCLUSIONS

Multi wall carbon nanotubes with a mean number of walls of 20 are grown via chemical vapour deposition directly on a stainless steel substrate. After characterization, the synthesized carbon nanostructures are airbrushed on a n-type silicon substrate to fabricate a simple photovoltaic device based on MWCNT/Si heterojunction. EQE response of the presented device is found to be correlated to the MWCNT film thickness. The optimum thickness value is  $240 \text{ k}\Omega/\text{cm}^2$ , where the resistance of the film is used to estimate the thickness. Our device shows a more efficient response in the near UV wavelength range, due to

the electron-hole pairs generation in the MWCNT film. This contribution is an advantage once the device will be competitive in terms of a better efficiency with the p-n junction solar cell. In particular, we believe that the efficiency of the presented device can be enhanced both by playing on the quality of the metallic contacts and by improving the homogeneity of the MWCNT film.

## REFERENCES

1. Castrucci P., Tombolini F., Scarselli M., Speiser E., Del Gobbo S., Richter W., De Crescenzi M., Diociaiuti M., Gatto E. and Venanzi M., *Appl. Phys. Lett.*, **89**(2006), 253107.
2. Barazzouk S., Hotchandani S., Vinodgopal K. and Kamat P. V., *Chem. B*, **108**(2004), 17015-8.
3. El Khakani M. A., Le Borgne V., Aissa B., Rosei F., Scilletta C., Speiser E., Scarselli M., Castrucci P. and De Crescenzi M., *Appl. Phys. Lett.*, **95**(2009), 083114
4. Wei J., Sun J.L., Zhu J.L., Wang K., Wang Z., Luo J., Wu D. and Cao A., *Small*, **2**(2006), 988-93.
5. Castrucci P., Scilletta C., Del Gobbo S., Scarselli M., Camilli L., Simeoni M., Delley B., Continenza A., De Crescenzi M., *Nanotechnology*, **22**(2011), 115701.
6. Le Borgne V., Castrucci P., Del Gobbo S., Scarselli M., De Crescenzi M., Mohamedi M., et al., *Appl. phys. Lett.*, **97**(2010), 193105-7.
7. Jia Y., Li P., Wei J., Cao A., Wang K., Li C., et al., *Res. Bull.*, **45**(2010), 1401-5.
8. Camilli L., Scarselli M., Del Gobbo S., Castrucci P., Nanni F., Gautron E., Lefrant S., De Crescenzi M., *Carbon*, **49**(2011), 3307-3315.
9. Dresselhaus M.S., Dresselhaus G., Saito R., Jorio A., *Phys. Rep.*, **409**(2005), 47-99.
10. Tuinstra F., Koenig J., *J Chem Phys.*, **53**(1970), 1126-30.
11. Ferrari A.C., Robertson J., *Phys., Rev. B*, **61**(2000), 14095-107.
12. Scarselli M., Castrucci P., Camilli L., Del Gobbo S., Casciardi S., Tombolini F., Gatto E., Venanzi M., De Crescenzi M., *Nanotechnology*, **22**(2011), 035701.
13. J. Nelson, 2003. *The Physics of Solar Cells*, Imperial College Press (London).